

Stopping Powers for Positrons and Electrons

W. N. Lennard, G. R. Massoumi, Peter J. Schultz, and P. J. Simpson

The Positron Beam Laboratory, Department of Physics, The University of Western Ontario, London, Ontario, Canada N6A 3K7

G. C. Aers

Institute for Microstructural Sciences, National Research Council of Canada, Ottawa, Ontario, Canada K1A 0R6

(Received 28 December 1994)

Stopping cross sections for 20 keV positrons (S^+) and electrons (S^-) in a thin ($61 \mu\text{g}/\text{cm}^2$) Al target have been measured using an electrostatic analyzer. The results yield a ratio $S^+/S^- = 1.15 \pm 0.08$, in good agreement with the theoretically calculated value of 1.097. A marked dependence of the mean energy loss on an emergence angle has been observed for a thin target, and its origin is interpreted with the aid of Monte Carlo simulations.

PACS numbers: 34.50.Bw, 34.80.Bm, 41.75.Fr, 87.50.Gi

Until now, measurements of positron (e^+) stopping powers have been hampered by the lack of availability of monoenergetic e^+ beams. Although a plenitude of energy loss data exist for electrons (e^-) in the 10–50 keV energy range, extraction of accurate stopping powers from the measurements is complicated by path-length enlargement effects in the case of direct measurements, or from the difficulty of accurate calorimetry (see Ref. [1] and references therein). Although measurements and theoretical work have spanned a period of almost 70 years, the subject remains of fundamental importance in radiological applications. It is still generally true that positron and electron stopping powers are calculated, rather than measured, using experimental I values (where I is the mean excitation energy) extracted from MeV proton stopping power data. Rohrlich and Carlson [2] showed that below 350 keV, positrons lose energy at a faster rate than electrons—an effect that originates from the indistinguishability of electrons in a binary collision wherein the faster of the two electrons is defined as the primary electron. For this reason, the maximum fractional energy transfers in Møller [3] (e^-e^-) and Bhabha [4] (e^+e^-) scattering are $\frac{1}{2}$ and 1, respectively. Thus, at energies ~ 20 keV, there should exist a measurable difference between the stopping powers for electrons and positrons; this difference should increase with the target Z value. Recently, Berger [5] has reviewed the differences between inelastic scattering cross sections for electrons and positrons.

Charged particles penetrating matter lose energy in a sequence of collisions with the constituent atoms of the medium. For the energy range considered here, the dominant collisional energy loss mechanisms are excitation and ionization of target atoms. (The ratio of radiative to collisional energy losses in Al is 3×10^{-4} and 7×10^{-4} for 20 keV e^+ and e^- , respectively [1].) The energy loss is primarily characterized by the stopping power [6]

$$-\frac{dE}{dR} = \lim_{R \rightarrow 0} \frac{\langle \varepsilon \rangle}{R}, \quad (1)$$

where $\langle \varepsilon \rangle$ is the mean energy loss after a traveled path length R . The stopping cross section, $S^\pm(E)$, given by Bohr's relation [7]

$$S^\pm(E) = \int T d\sigma^\pm(E, T), \quad (2)$$

where $d\sigma^\pm(E, T)$ is the positron-electron (+) or electron-electron (–) cross section for energy transfer T at energy E . Since $S = (1/N) dE/dR$ then $\langle \varepsilon^\pm \rangle = NRS^\pm(E)$ for a sufficiently short path length R , where N is the target atom density. In practice, dE/dR or S^\pm can be derived from $\langle \varepsilon^\pm \rangle$ when the measurements include *all* transmitted particles. We stress that the results must be corrected for path-length enlargement effects arising from scattering in the target.

In this work, we report results for $S^\pm(E)$ deduced from measurements of energy loss distributions as a function of emergence angle θ for both e^+ and e^- after traversing a thin Al target at an incident energy of 20 keV. The ratio of the stopping cross sections for e^+ and e^- is determined and compared with theory. Finally, the measured e^+ energy loss distribution is compared to the Landau distribution [8] as modified by Blunck and Leisegang [9] and Seltzer [10].

Experiments were performed using the University of Western Ontario electrostatically guided positron beam, which is described elsewhere [11]. Briefly, transmitted energy distributions were measured for monoenergetic e^+ and e^- incident at 20.4 keV on a $61(\pm 2) \mu\text{g}/\text{cm}^2$ self-supporting Al foil using a high energy resolution electrostatic analyzer (ESA, $\Delta E/E = 1.5\%$) that was rotatable to span the region $\theta = 0^\circ - 60^\circ$ and subtended a solid angle of ~ 1 msr. The spread in beam energy from the source was < 3 eV for both positrons and electrons, and the short term (~ 1 h) stability of the Glassman high voltage power supply was 0.01%, e.g., 2 eV for a 20 keV beam energy. Fluctuation in the particle energies as measured by the ESA were ~ 5 eV over several days, which confirms the above estimates. The relative transmitted particle intensities, $I(\theta)$ (integrated over azimuthal

angle), were determined using frequent “target out” measurements to record the incident beam intensity. Measurements were performed for emergence angles $\theta \leq 28^\circ$ due to limitations in the signal intensity for larger angles. The measured mean energy loss was then obtained via $\langle \varepsilon^\pm \rangle = \sum I^\pm(\theta) \langle \varepsilon^\pm(\theta) \rangle / \sum I^\pm(\theta)$.

The Al target thickness, chosen to keep the mean projectile energy loss in the target small, i.e., $\langle \varepsilon^\pm \rangle / E_0 < 4\%$, was measured by Rutherford backscattering (RBS) using 1 MeV $^4\text{He}^+$ incident ions. The RBS measurement was made absolute using a calibrated ^{209}Bi -implanted Si target for comparison [12]. No evidence for Al target crystallinity was observed in the RBS measurements, thereby assuring that channeling effects on the e^\pm measurements were insignificant. Target thickness values before and after the e^\pm measurements were identical.

A Monte Carlo scheme has been previously developed to simulate trajectories for e^+ traversing elemental targets [13–15], yielding energy distributions as a function of angle for both backscattered and transmitted projectiles. Here inelastic scattering was described within the dielectric formalism using the model dielectric function proposed by Penn [16] with experimental optical data. From these simulations, it was found that $\sim 82\%$ of the transmitted particles were contained in the forward direction out to $\theta = 28^\circ$, i.e., the angular region spanned by the data. In all cases, the transmitted mean energy $\langle E(\theta) \rangle$ was obtained by integrating the measured projectile energy spectrum observed at angle θ , thereby yielding $\langle \varepsilon(\theta) \rangle = E_0 - \langle E(\theta) \rangle$. In order to deduce the mean energy loss for all particles, the $\langle \varepsilon^\pm(\theta) \rangle$ data were summed with appropriate weighting factors reflecting the measured angular intensities to yield values for S^\pm . Using simulated energy spectra convoluted with ESA resolution, it was confirmed that $\langle \varepsilon \rangle$ was unchanged by the convolution at the 10^{-6} level.

Electron and positron mean energy losses as a function of scattering angle $\langle \varepsilon^\pm(\theta) \rangle$ are shown in Fig. 1. $\langle \varepsilon^+ \rangle$ is larger than $\langle \varepsilon^- \rangle$ at all angles. For both projectile types, $\langle \varepsilon \rangle$ increases markedly with increasing angle θ , which is attributable to two effects. First, there is the trivial path-length enlargement which arises from projectile scattering within the target. Second, and more important, those particles exiting the foil near $\theta \approx 0^\circ$ have not suffered large angle collisions (in the classical sense) with atomic electrons, thereby precluding large inelastic losses, as the probability to rescatter into the 0° direction is small for thin foil targets. While it is still true that the angular intensity is dominated by elastic collisions with the atomic nuclei, the mean energy loss (for thin targets) *cannot* be extracted from a measurement near 0° with a restricted solid angle, since the integral over all inelastic energy transfers, as required to determine experimentally a value for the expression $\int T d\sigma(T)$ [cf. Eq. (2)], is incomplete. Note that the dependence of the mean-square scattering angle on the nuclear charge Z follows from $\langle \theta^2 \rangle \propto Z(Z +$

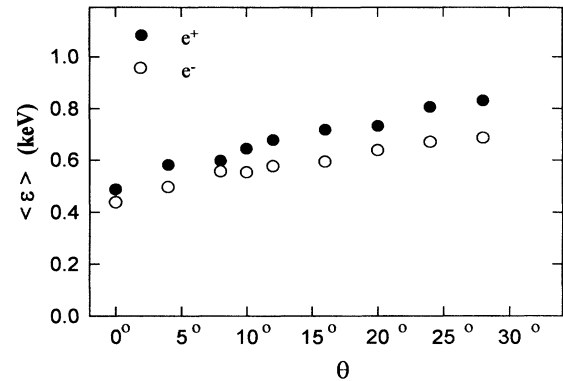


FIG. 1. Mean energy loss $\langle \varepsilon^\pm(\theta) \rangle$ as a function of angle for incident 20.4 keV positrons and electrons transmitted through a $61 \mu\text{g}/\text{cm}^2$ Al foil. The uncertainty for each measured value is $\sim 5\%$.

1) [17]. An angular deflection of the projectile by a target electron has a cross section that is smaller by a factor of Z^2 from the Rutherford cross section for scattering from the nucleus, but there are Z electrons per atom.

To obviate the effect of average path-length enlargement $\langle \Delta \rangle$ due to angular scattering, two approaches were considered: (1) $\langle \Delta \rangle / R$ was calculated at each angle using the Monte Carlo simulation; (2) $\langle \Delta \rangle / R$ was calculated using the method suggested by Yang [18] (see also Hubbell and Birkhoff [19]), where

$$\langle \Delta \rangle = \frac{1}{2} \int_0^R \langle \theta^2(t) \rangle dt. \quad (3)$$

Here $\langle \theta^2(t) \rangle$ as a function of target thickness t was obtained from Ref. [17]. In determining the total energy loss spectrum for all particles, we find an average fractional path-length enlargement $\langle \Delta \rangle / R = 0.065$ from the Monte Carlo simulation. Using method (2), we find $\langle \Delta \rangle / R = 0.048$. Actually, $\langle \Delta \rangle / R$ was found to increase monotonically with θ , from 0.0043 at $\theta = 0^\circ$ to 0.072 at $\theta = 28^\circ$.

The e^+ and e^- relative angular intensities $I(\theta)$ measured for the $61 \mu\text{g}/\text{cm}^2$ Al target at 20.4 keV are shown in Fig. 2, where the experimental data are normalized to have the same integral. There is good agreement between the experimental angular intensities and the e^+ Monte Carlo simulations for all scattering angles. The value for the mean e^+ scattering angle $\langle \theta^2 \rangle^{1/2}$, is found to be 23.5° for the Monte Carlo simulation, compared to the value 25.1° derived from the results of Ritchie, Ashley, and Emerson [17] for electrons. The measured angular intensities are also similar for e^+ and e^- , as expected for low- Z targets at $E = 20$ keV. For all θ , $d\sigma^-/d\theta \geq d\sigma^+/d\theta$, but the difference (for $\sin \theta \neq 0$) decreases monotonically with diminishing velocity [2]. Even at 400 keV, the fractional difference observed in the angular widths for positron-electron multiple scattering was only $\sim 1.2\%$ [20] for Al targets.

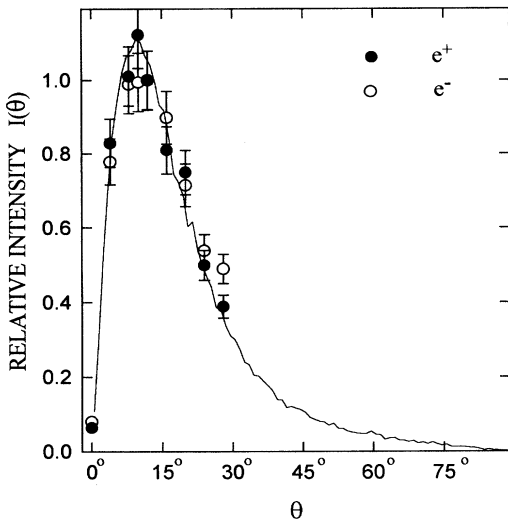


FIG. 2. Measured relative angular intensities $I^\pm(\theta)$ for both positrons and electrons transmitted through the Al foil. The solid line is the result of a Monte Carlo calculation for positrons. All data are normalized to have the same integral.

A correction to the data has been incorporated using the results of Monte Carlo simulations for positrons to account for the omission of those particles scattered to angles exceeding 28° . We have extrapolated the e^+ and e^- measured energy losses using those data with $\theta \leq 28^\circ$ (see Fig. 1) assuming a linear dependence of $\langle \varepsilon(\theta) \rangle$ on θ (out to $\theta = 76^\circ$, which then includes 99.7% of all transmitted particles). $\langle \varepsilon \rangle$ is then found to increase by 3.3% for e^+ and 2.2% for e^- (after correcting for the path-length enlargement effect). This correction has the effect of increasing the ratio of stopping cross sections, S^+/S^- , by only 1% since only a small fraction ($\sim 18\%$) of the total transmitted particles were excluded from the measurements.

An analysis of the e^\pm energy loss data yields values $S^+ = 11.0 \pm 0.7 \text{ MeV cm}^2 \text{ g}^{-1}$ and $S^- = 9.56 \pm 0.6 \text{ MeV cm}^2 \text{ g}^{-1}$, compared with calculated values [1] of 10.75 and 9.81 $\text{MeV cm}^2 \text{ g}^{-1}$, respectively. Thus, the experimental ratio is $S^+/S^- = 1.15(\pm 0.08)$ at 20.1 keV ($= E_0 - \langle \varepsilon \rangle / 2$). The error estimate for the ratio does not include the absolute uncertainty in the Al target thickness since the identical target and geometry were used for all e^+ and e^- energy loss measurements. According to the most recent compilation [1], the calculated ratio is $S^+/S^- = 1.097$ using an I value of 166 eV and a density effect correction $\delta = 1.031 \times 10^{-3}$. The present measurement is in good agreement with the theoretically calculated value.

The total energy loss distribution measured for incident positrons is shown in Fig. 3 (for $\theta \leq 28^\circ$). The smooth curve is a calculation assuming the Landau distribution with the width modified according to Blunck and Leisegang [9], following Seltzer's prescription [10]; the

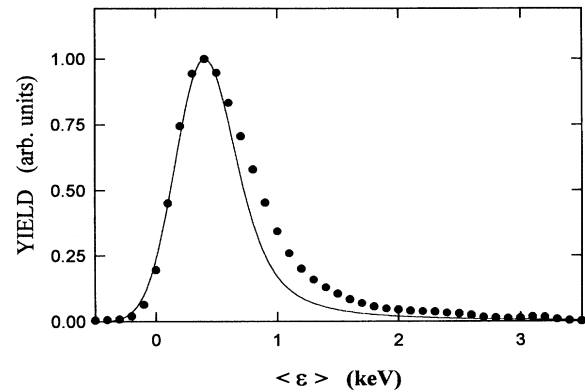


FIG. 3. Measured energy loss distribution for e^+ projectiles transmitted through a $61 \mu\text{g}/\text{cm}^2$ Al foil with θ values $\leq 28^\circ$. The smooth curve is a calculation following the method of Seltzer [10], including a convolution with the ESA resolution function.

ESA resolution has been folded in to facilitate comparison with the experimental data. In the calculation, we have used a target thickness that is 2% larger than the measured value to account for the average path-length enhancement for those particles transmitted with $\theta \leq 28^\circ$. The measured most probable energy loss ε_p is in reasonable agreement with the calculated value. The positron energy loss straggling, estimated from the FWHM of the distribution and corrected for the ESA resolution, has a value ~ 0.68 keV. In general, the calculated and measured curves are concordant.

Cosslett and Thomas [21] have measured $\langle \varepsilon(\theta) \rangle$ for 15 keV electrons in Al using thicker targets, where little or no dependence of $\langle \varepsilon \rangle$ on θ was observed. Their mean energy loss data as a function of angle are supported by our Monte Carlo results (for positrons), which show that as the foil thickness increases, all transmitted particles exhibit nearly the same mean energy loss due to a large number of inelastic collisions. As well, in this case the angular intensity becomes only weakly θ dependent.

Schneider *et al.* [22] have recently reported e^\pm energy loss data in the range 5–15 keV from measurements made in the forward direction. Their results suggest a marked disagreement with theory [1] in that $S^+ < S^-$, which is also in conflict with the present data. In light of the discussion concerning the relation between the energy and emergent angle, those data should be regarded circumspectly. In general, correlations between (electronic) energy loss and scattering cannot be ignored; the energy loss must have a minimum for zero emergence angle [6], and it is not possible to sample properly the energy loss distribution via measurements restricted to small forward angles. An analogous consideration arises in the treatment of stopping powers for heavy ions (e.g., protons) using the local density approximation [23]. If we compare our values for $\langle \varepsilon^\pm(0^\circ) \rangle$, i.e., the

mean energy losses measured at 0° , we find a ratio $\langle \varepsilon^+(0^\circ) \rangle / \langle \varepsilon^-(0^\circ) \rangle = 1.11 \pm 0.08$, but the absolute values of $\langle \varepsilon^+(0^\circ) \rangle$ and $\langle \varepsilon^-(0^\circ) \rangle$ are $\sim 30\%$ smaller than the values $\langle \varepsilon^\pm \rangle$ obtained by integrating over all angles.

In conclusion, the mean energy losses $\langle \varepsilon \rangle$, measured for 20 keV e^+ and e^- , are in good agreement with theoretical predictions for a $Z = 13$ target and measured energy loss spectra for positrons are in excellent agreement with those predicted by Monte Carlo simulations. In order to obtain accurate values for S^\pm using a thin target where a marked angle dependence of the mean energy loss has been observed, it was necessary to record data over a wide range of emergence angles and to subsequently correct for path-length enlargement arising from scattering within the target. However, the ratio S^+/S^- was largely insensitive to the latter correction. Further, measurements at lower projectile energies and for higher- Z targets, where the deviations of S^+/S^- from unity are predicted to be larger than for Al, should provide confirmation of the phenomena reported in this work.

The authors are grateful for the technical assistance of I. Schmidt, B. Campbell, and P. Perquin. Funding for this research has been provided by the Natural Sciences and Engineering Research Council (NSERC) of Canada.

-
- [1] International Commission on Radiation Units and Measurements Report No. ICRU 37, 1984 (unpublished).
 - [2] F. Rohrlich and B. C. Carlson, *Phys. Rev.* **98**, 38 (1954).
 - [3] C. Møller, *Ann. Phys. (Leipzig)* **14**, 531 (1932).
 - [4] H. J. Bhabha, *Proc. R. Soc. London A* **154**, 195 (1936).
 - [5] M. J. Berger, *Appl. Radiat. Isot.* **42**, 905 (1991).

- [6] P. Sigmund, *Nucl. Instrum. Methods Phys. Res. Sect. B* **12**, 1 (1985).
- [7] N. Bohr, *Mat. Fys. Medd. K. Dan. Vidensk. Selsk.* **18**, No. 8 (1948).
- [8] L. Landau, *J. Phys. USSR* **8**, 201 (1944).
- [9] O. Blunck and S. Leisegang, *Z. Phys.* **128**, 500 (1950).
- [10] S. M. Seltzer, *Appl. Radiat. Isot.* **42**, 917 (1991).
- [11] G. R. Massoumi, N. Hozhabri, W. N. Lennard, P. J. Schultz, S. F. Baert, H. H. Jorch, and A. H. Weiss, *Rev. Sci. Instrum.* **62**, 1460 (1991).
- [12] T. E. Jackman, J. A. Davies, and D. Chivers, *Nucl. Instrum. Methods Phys. Res. Sect. B* **19/20**, 345 (1987).
- [13] G. R. Massoumi, N. Hozhabri, K. O. Jensen, W. N. Lennard, M. S. Lorenzo, P. J. Schultz, and A. B. Walker, *Phys. Rev. Lett.* **68**, 3873 (1992).
- [14] G. R. Massoumi, W. N. Lennard, P. J. Schultz, A. B. Walker, and K. O. Jensen, *Phys. Rev. B* **47**, 11007 (1993).
- [15] K. O. Jensen and A. B. Walker, *Surf. Sci.* **292**, 83 (1993).
- [16] D. R. Penn, *Phys. Rev. B* **35**, 482 (1987).
- [17] R. H. Ritchie, J. C. Ashley, and L. C. Emerson, *Phys. Rev.* **135**, A759 (1964).
- [18] C. N. Yang, *Phys. Rev.* **84**, 599 (1951).
- [19] H. H. Hubbell, Jr. and R. D. Birkhoff, *Phys. Rev. A* **26**, 2460 (1982).
- [20] B. P. Nigam and V. S. Mathur, *Phys. Rev.* **121**, 1577 (1961).
- [21] V. E. Cosslett and R. N. Thomas, *Br. J. Appl. Phys.* **15**, 883 (1964).
- [22] H. Schneider, I. Tobehn, M. Rückert, U. Brinkman, and R. Hippler, *Nucl. Instrum. Methods Phys. Res. Sect. B* **79**, 353 (1993).
- [23] H. H. Mikkelsen and P. Sigmund, *Nucl. Instrum. Methods Phys. Res., Sect. B* **27**, 266 (1987).